Polarization dependence of a GaAs-based two-photon absorption microcavity photodetector

J. O' Dowd,[1,*] W. H. Guo,[1] E. Flood,[1] M. Lynch,[1] A. L. Bradley,[1] L. P. Barry,[2] and J. F. Donegan[1]

[1]*Semiconductor Photonics Group, School of Physics, and Centre for Telecommunication Value-Chain Research (CTVR), Trinity College, Dublin 2, Ireland*
[2]*RINCE, School of Electronics Engineering, Dublin City University, Dublin 9, Ireland*
[*]*Corresponding author: jodowd@tcd.ie*

Abstract: In this paper, the polarization response of a GaAs based two-photon absorption microcavity photodetector has been studied. The deviation in the dependence of the detector response from that of bulk GaAs is shown to be due to the birefringence of the cavity. A theoretical model based on the convolution of the cavity birefringence and the polarization dependence of two-photon absorption in GaAs is described and shown to match the measured polarization dependence of the microcavity detector very well.

OCIS codes: (190.4360) Non linear optics, devices; (190.4180) Multiphoton processes; (230.5440) Polarization-selective devices.

References and links

1. J. K. Ranka, A. L. Gaeta, A. Baltuska, M. S. Pshenichnikov, and D. A. Wiersma, "Autocorrelation measurement of 6-fs pulses based on the two-photon-induced photocurrent in a GaAsP photodiode," Opt. Lett. **22**, 1344-1346 (1997).
2. S. Wielandy, M. Fishteyn, and B. Zhu, "Optical performance monitoring using nonlinear detection," J. Lightwave Technol. **22**, 784-793 (2004)
3. P. J. Maguire, L. P. Barry, T. Krug, M. Lynch, A. L. Bradley, J. F. Donegan, and H. Folliot, "All-optical sampling utilising two-photon absorption in semiconductor microcavity," Electron. Lett. **41**, 489-490 (2005).
4. R. Salem and T. E. Murphy, "Broad-band optical clock recovery system using two-photon absorption," IEEE Photon. Technol. Lett. **16**, 2141-2143 (2004).
5. B J. M. Roth, T. E. Murphy, and C. Xu, "Ultrasensitive and high-dynamic-range two-photon absorption in a GaAs photomultiplier tube," Opt. Lett. **27**, 2076-2078 (2002).
6. C. Xu, J. M. Roth, W. H. Knox, and K. Bergman, "Ultra-sensitive autocorrelation of 1.5 μm light with single photon counting silicon avalanche photodiode," Electron. Lett. **38**, 86-88 (2002).
7. T. K. Liang, H. K. Tsang, I. E. Day, J. Drake, A. P. Knights, and M. Asghari, "Silicon waveguide two-photon absorption detector at 1.5 μm wavelength for autocorrelation measurements," Appl. Phys. Lett. **81**, 1323-1325 (2002).
8. Y. Jing Yong, M. Ishikawa, Y. Yamane, N. Tsurumachi, and H. Nakatsuka, "Enhancement of two-photon excited fluorescence using one-dimensional photonic crystals," Appl. Phys. Lett. **75**, 3605 (1999).
9. H. Folliot, M. Lynch, A. L. Bradley, L. A. Dunbar, J. Hegarty, J. F. Donegan, L. P. Barry, J. S. Roberts, and G. Hill, "Two-photon absorption photocurrent enhancement in bulk AlGaAs semiconductor microcavities," Appl. Phys. Lett. **80**, 1328-1330 (2002).
10. T. Krug, W. H. Guo, J. O'Dowd, M. Lynch, A. L. Bradley, J. F. Donegan, P. J. Maguire, L. P. Barry, and H. Folliot, "Resonance tuning of two-photon absorption microcavities for wavelength-selective pulse monitoring," IEEE Photon. Technol. Lett. **18**, 433-435 (2006).
11. W. H. Guo, J. O'Dowd, M. Lynch, A. L. Bradley, J. F. Donegan, and L. P. Barry, "Influence of cavity lifetime on high-finesse microcavity two-photon absorption photodetectors," IEEE Photon. Technol. Lett. **19**, 432-434 (2007).
12. D. C. Hutchings and B. S. Wherrett, "Theory of anisotropy of two-photon absorption in zinc-blende semiconductors," Phys. Rev. B **49**, 2418 (1994).
13. M. D. Dvorak, W. A. Schroeder, D. R. Andersen, A. L. Smirl, and B. S. Wherrett, "Measurement of the anisotropy of two-photon absorption coefficients in zincblende semiconductors," IEEE J. Quantum Electron. **30**, 256-268 (1994).
14. W. H. Guo, J. O'Dowd, E. Flood, M. Lynch, A. L. Bradley, J. F. Donegan, K. Bondarczuk, P. J. Maguire, and L. P. Barry, "Suppression of residual single-photon absorption relative to two-photon absorption in high finesse planar microcavities," IEEE Photon. Technol. Lett. (accepted for publication).

#98727 - $15.00 USD Received 11 Jul 2008; revised 6 Oct 2008; accepted 6 Oct 2008; published 17 Oct 2008

15. M. P. van Exter, A. K. Jansen van Doorn, and J. P. Woerdman, "Electro-optic effect and birefringence in semiconductor vertical-cavity lasers," Phys. Rev. A **56**, 845 (1997).

1. Introduction

Two-photon absorption (TPA) in semiconductors has recently received much attention as a means of carrying out a variety of pulse characterization techniques. The auto-correlation of pulses as short as 6 fs has been reported using TPA detectors [1]. TPA applications in optical telecommunications networks have also been demonstrated, such as optical performance monitoring [2], optical sampling [3] and optical clock recovery [4].

As TPA is a weak, non-linear process, a suitable detector structure or very tight focusing must be chosen to enable use at low input optical power. Improved responses have previously been reported for a number of different types of detectors such as photomultiplier tubes [5], silicon avalanche photodiodes [6] and in waveguides [7]. Resonant enhancement of two-photon excited fluorescence in one-dimensional photonic crystals has been shown in [8], and TPA enhancement in microcavities has been demonstrated by our group [9].

In this paper, the polarization dependence of TPA in a GaAs/AlAs microcavity enhanced TPA detector is investigated. The microcavity detector consists of a bulk GaAs absorption region sandwiched between two distributed Bragg reflectors (DBR's). Previously, TPA enhancement of greater than 10,000 has been reported by our group, due to enhancement of the electric field in the absorption region once the resonance criteria of the structure has been satisfied [9]. Compared with other TPA detectors, the microcavity has the added advantage of having an integrated filter with a spectral width that can be selected by changing the reflectivity of the Bragg mirrors. The peak transmission of this filter response is angle tunable over a range greater than 35 nm [10]. In addition, the microcavity can be optimized for particular pulse durations by varying the Bragg mirror reflectivity, which in turn changes the cavity lifetime [11].

In order to use these structures for TPA applications in which the polarization of the input signal is subject to change, we must first fully understand the TPA polarization dependence in these microcavities. The polarization dependence of the TPA coefficient is dependant on the crystalline orientation of the material [12]. The polarization dependence of TPA in (001) GaAs at 950 nm has been previously reported in [13]. As a linear polarization is rotated through 360 degrees, the TPA dependence is periodic, with a period of 90 degrees, and a variation of approximately 27 % in the TPA coefficient (β). For the microcavity the polarization dependence of the TPA process and the microcavity itself are convoluted. It is therefore necessary to characterize the additional contribution of the cavity effect to the intrinsic polarization dependence of bulk GaAs.

2. Theory and experiment

TPA measurements were carried out using a $Ga_{0.1}Al_{0.9}As/Ga_{0.88}Al_{0.12}As$ microcavity which is resonant at λ = 1561 nm with a 1 λ thick GaAs absorption region. The cavity has 7 p-doped top mirror pairs and 24 n-doped bottom mirror pairs which optimize the cavity for pulses of 2 ps in duration [11]. The input optical signal is provided by an external cavity tunable diode laser which is modulated at 300 kHz with a duty cycle of 50 %. The signal is amplified by an erbium-doped-fiber-amplifier (EDFA) so as to allow the TPA-dominated regime to be accessed. The signal is also passed through a variable optical attenuator and a polarization controller. The polarization controller consists of an input polarizer and a half- and quarter-wave plate. Using the polarization controller, the specific polarization of the input signal onto the detector can be set. The detector is placed away from the in-focus position so as to reduce the effect of angular components of the input beam, which can result in asymmetry of the measured TPA spectrum due to the angular dependence of the microcavity response.

#98727 - $15.00 USD Received 11 Jul 2008; revised 6 Oct 2008; accepted 6 Oct 2008; published 17 Oct 2008

The TPA microcavity photodetector also has some residual single-photon absorption (SPA) which is also enhanced by the microcavity [14]. The SPA polarization dependence of the microcavity photodetector was investigated first. The polarization state of the input signal was rotated through various states of linear polarization around the Poincaré sphere; see Fig. 1. These scans were carried out with the average power held constant at 0.15 mW, which is low enough for the detected photocurrent to be dominated by SPA, as shown in Fig. 2(inset), which shows the microcavity detector photocurrent as a function of incident power near the cavity resonance. The graph is plotted with a log-log scale on which a slope of two and slope of one correspond to the TPA and SPA dominant regimes, respectively. For bulk GaAs, SPA is independent of the linear polarization state but as can be seen in Fig. 1 there is a clear polarization dependence of the detected photocurrent. The deviation from the bulk material response can be explained by the birefringence of the cavity with the minimum and maximum of the SPA polarization dependence corresponding to the two eigenmodes of the cavity. Similar birefringence has previously been seen in vertical-cavity-surface-emitting-lasers (VCSEL's) which are similar in structure to these microcavities [15]. The eigenmodes are assumed to correspond to linear polarization states polarized in the [110] and $[1\bar{1}0]$ crystallographic directions [15].

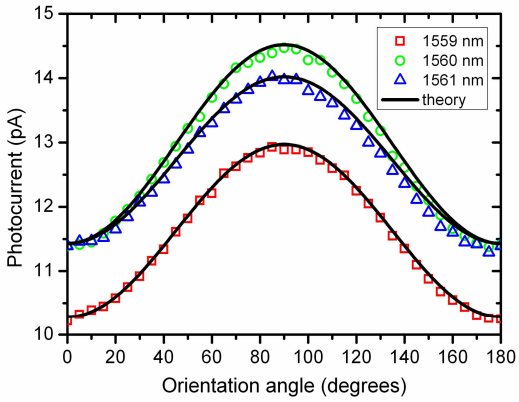

Fig. 1. SPA generated photocurrent vs. orientation of linear state of polarization (θ) of the incident optical signal. The polarization scan is carried out at a low average power (0.15 mW) in the SPA dominant regime at three different wavelengths around the cavity resonance.

The wavelength dependence of the photocurrent for states of polarization corresponding to the two eigenmodes is shown in Fig. 2. The peak SPA photocurrent exhibits a 0.15 nm splitting between the two eigenmodes, providing a further indication of the birefringence of the cavity. Also these two eigenmodes have very different quality factors, as can be seen from the differences in their spectral widths. These spectral scans were repeated with a high average incident power of 37.8 mW, corresponding to the TPA-dominant regime, as can be seen in the inset of Fig. 2, and a similar splitting in the TPA response is observed.

Further investigation of the polarization dependence of the microcavity photocurrent was performed by scanning the state of polarization from circular through linear and back to circular in the SPA dominant regime, as shown in Fig. 3. SPA in bulk GaAs has no phase dependence, so the change in SPA photocurrent in Fig. 3 can again be explained by the birefringence of the cavity. As the ellipticity of the signal changes, so too does the ratio of the power coupled into each eigenmode. The cavity enhances the two eigenmodes differently, resulting in the polarization dependence seen in Fig. 3. It has been previously reported in similar VCSEL structures that such a splitting is primarily attributable to the electro-optic effect, due to internal fields at the material junctions in the DBR's as well as a smaller contribution from strain associated with growth and processing [15].

#98727 - $15.00 USD Received 11 Jul 2008; revised 6 Oct 2008; accepted 6 Oct 2008; published 17 Oct 2008

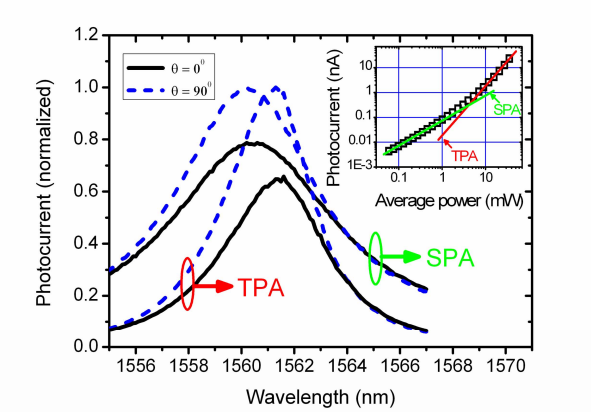

Fig. 2. Normalized photocurrent vs. wavelength for both high average power incidence and low average power incidence, corresponding to the TPA and SPA dominant regimes, respectively. The wavelength scans were carried out for the linear polarization states corresponding to the peak ($\theta = 90^0$) and trough ($\theta = 0^0$) of Fig. 1. Fig. 2(inset). Photocurrent vs. incident optical power curve carried out near the resonant wavelength.

The SPA polarization dependence of the microcavity can be found by calculating the enhancement by the microcavity for the two cavity eigenmodes. Once the enhancement of each of the modes is known, the SPA response of the microcavity for all input polarization states can be calculated. In order to characterize the enhancement of the cavity, the overall reflectivity of the cavity (R) for each of the eigenmodes must be determined. This can be calculated from the SPA photocurrent spectra in Fig. 2. By fitting the spectral response of each of the two eigenmodes with a Lorentzian function, we can extract the bandwidth (BW) and the resonant wavelength (λ_0). The free spectral range (FSR) is given by $FSR=\lambda_0/2D$ where D is the effective optical cavity length and is theoretically calculated to be 1.97 μm [14]. R can now be calculated using $BW / FSR = R^{-1/2}(1-R)/\pi$ and the cavity field enhancement factor is given by

$$e_{x,y} = \frac{C_{x,y}}{1 - R\exp\left[-i\frac{2\pi\Delta\lambda_{x,y}}{FSR}\right]} \qquad (1)$$

which describes the field in the cavity relative to the input electric field. $\Delta\lambda$ is the deviation of the wavelength being investigated from the resonant wavelength of the cavity which is used to determine the phase change with wavelength, which changes by 2π when the wavelength changes by one FSR. The SPA photocurrent generated in the TPA microcavity is described by $I_{SPA} = \alpha A|e|^2$, where α is the SPA absorption coefficient and A is a constant; both parameters are polarization independent. The unknown polarization dependent parameter $C_{x,y}$ in (1) can be calculated by fitting the SPA photocurrent calculated from (1) to the data in Fig. 1 for each of the two eigenmodes ($\theta = 0^\circ$ and 90° respectively). The full SPA linear polarization dependence of the cavity can be calculated for all states of linear polarization by calculating the amount of power coupled to each of the eigenmodes and then taking into account the relative enhancement of each mode using (1), as can be seen in Fig. 1. Similarly, it is possible to fit the polarization dependence of the cavity for all elliptical polarizations, as there is no phase dependence for SPA in bulk GaAs. Once the power coupled into each eigenmode has been calculated, using (1) the SPA generated photocurrent for that polarization state can be calculated, the results of which are shown in Fig. 3. As seen from both Fig. 1 and Fig. 3, the theoretical results based on the above analysis agree very well with the experimental data, which suggests that the previous assumption that both eigenmodes are linearly polarized, and their orientations are related to the peak and trough of Fig. 1, is valid.

#98727 - $15.00 USD Received 11 Jul 2008; revised 6 Oct 2008; accepted 6 Oct 2008; published 17 Oct 2008

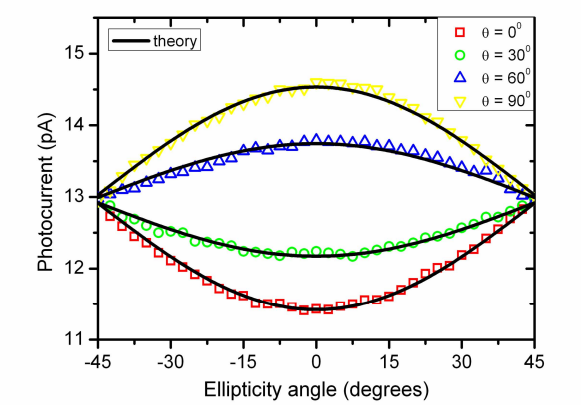

Fig. 3. Dependence of the SPA photocurrent on the state of polarization as it is rotated from circular to linear to circular along a 4 different longitudinal lines of the Poincaré sphere, where θ is the orientation angle.

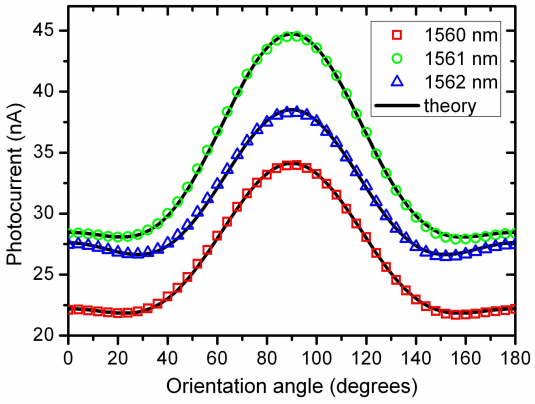

Fig. 4. TPA photocurrent vs. orientation of the linear state of polarization of the incident optical signal, recorded for three wavelengths around the cavity resonance.

The case for TPA is slightly more complicated, as the TPA process in GaAs is polarization dependant. From Fig. 2 it can be seen that the resonance wavelength of the cavity is not the same for the TPA dominated regime as it is in the SPA dominated regime. This can be explained by the thermal tuning of the cavity because of the large difference in incident power levels used for the TPA and SPA dominant regimes. The dependence of TPA photocurrent on the orientation of the linear polarization state was recorded at three wavelengths around the cavity resonance, with constant average power incident, as shown in Fig. 4. The local maxima ($\theta = 0^{\circ}$ and 90°) correspond to the eigenmodes of the cavity. The difference between the amplitudes of the peaks is due to the birefringence of the cavity. In the absence of birefringence, the amplitude of both peaks would be the same for all wavelengths. The TPA photocurrent was also recorded as the input polarization state was scanned from circular to linear to circular along four different longitudinal axes of the Poincaré sphere, see Fig. 5.

In order to model the polarization dependence of the TPA photocurrent, we must first calculate the intrinsic polarization dependence of TPA in GaAs and then couple it with the polarization dependence of the cavity as described for the SPA case. The TPA-generated photocurrent in the microcavity can be described by $I_{TPA} = \beta B|e|^4$, where β is the TPA absorption coefficient in the microcavity and B is a polarization independent constant. The polarization dependence of TPA in GaAs has previously been described in [12] as being

#98727 - $15.00 USD Received 11 Jul 2008; revised 6 Oct 2008; accepted 6 Oct 2008; published 17 Oct 2008

dependant on three parameters. These are $\chi^{''}_{xxxx}$, σ the anisotropy parameter, where $\sigma = [\chi^{''}_{xxxx} - \chi^{''}_{xxyy} - 2\chi^{''}_{xyxy})]/\chi^{''}_{xxxx}$ and δ, which is the incremental TPA dichroism parameter, where $\delta = [\chi^{''}_{xxxx} + \chi^{''}_{xxyy} - 2\chi^{''}_{xyxy}]/2\chi^{''}_{xxxx}$. χ is a 4th rank tensor that describes the 3rd order susceptibility of GaAs, where $\chi^{''}_{xxxx}$ is used as a shorthand representation of $Im\,\chi^{''}_{xxxx}(-\omega,\omega,\omega)$, etc. The value for σ in GaAs has been previously reported as –0.76 at 950 nm [13]. The value at 1550 nm has not previously been measured experimentally, but the theoretical value is approximately half the value reported at 950 nm value [12]. Similarly, a value for δ has not previously been measured at 1550 nm. Both σ and δ at 1550 nm are determined later in this paper. Using these parameters β can be expressed in a form similar to that used in [13]:

$$\beta = \frac{\omega}{2n^2c^2\varepsilon_0}\chi^{''}_{xxxx}\left(\left(\frac{2-\sigma-2\delta}{2}\right)+\left(\frac{2\delta-\sigma}{2}\right)\left|\hat{\zeta}.\hat{\zeta}\right|^2+\sigma\sum_i\left|\zeta_i^4\right|\right) \tag{2}$$

where $\hat{\zeta}$ is the Jones matrix describing the polarization state with reference to the principal crystallographic axes of GaAs. In order to calculate the TPA photocurrent, the electric field inside the cavity has to be found first using (1), by decomposing the incident polarization into two orthogonal directions based on the two eigenmodes of the cavity. This is similar to the process used for the SPA photocurrent calculation. The Jones matrix describing the polarization state inside the cavity was then determined. To facilitate the use of (2) in calculating the TPA photocurrent, the Jones matrix is rotated by 45 degrees, as the eigenmodes are oriented along [110] and $[1\bar{1}0]$ directions.

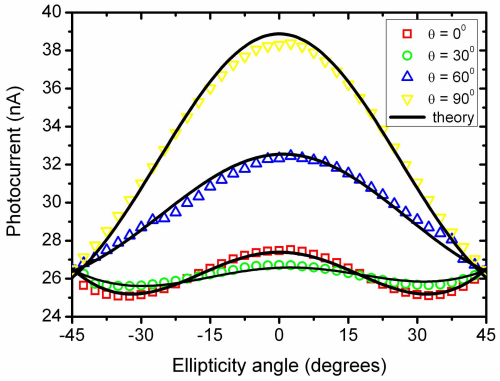

Fig. 5. Dependence of the TPA photocurrent on the state of polarization as it is rotated from circular to linear to circular along 4 different longitudinal lines of the Poincaré sphere, where θ is the orientation angle.

As in the SPA case, the polarization dependent parameter $C_{x,y}$ was found experimentally by fitting the calculated photocurrent to the linear polarization states corresponding to the two eigenmodes; see Fig. 4. The calculated $C_{x,y}$ values are then used in calculations for all the other states of polarization. The mode splitting of the two eigenmodes is very small when compared with the spectral width, as shown in Fig. 2. This shows that once the incident polarization is linear, the polarization inside the cavity does not significantly gain ellipticity, but its orientation will be changed slightly due to the enhancement difference of each of the eigenmodes. As the polarization remains linear, the change in the TPA coefficient will be dependent only on σ which can be determined by fitting the measured linear polarization dependence in Fig. 4. We find that an excellent fit can be achieved for a value of σ equal to –0.33, as seen in Fig. 4.

#98727 - $15.00 USD Received 11 Jul 2008; revised 6 Oct 2008; accepted 6 Oct 2008; published 17 Oct 2008

As the incident polarization gains ellipticity, the electric field inside the cavity can still be found through processes similar to those introduced above; however the polarization inside the cavity will be elliptical as well. For elliptical polarizations, the TPA coefficient will also depend on δ. With the value for σ obtained above and using δ as a fitting parameter, we can repeat the above fitting process on the measured curves in Fig. 5. As can be seen in Fig. 5, an excellent fit can be achieved for a value of δ equal to 0.068. The values calculated here of σ = -0.33 and δ = 0.068 are similar to the theoretical values predicted by [12], which are σ = -0.487 and δ = 0.076 and were obtained using low temperature parameters of GaAs. Although the values reported in this paper were obtained at room temperature, they are still in good agreement with the values reported in [12].

3. Conclusion

A full characterization of the polarization dependence of TPA and SPA in a GaAs-based microcavity photodetector has been carried out. The two eigenmodes of the cavity have been identified and shown to be separated by 0.15 nm, due to birefringence in the cavity. The effect of this birefringence on the field enhancement associated with the two cavity eigenmodes has been shown to explain the deviation of the polarization dependence of the microcavity structure from that of bulk GaAs. In order to characterize the polarization dependence of the TPA photocurrent in the microcavity detector, experimental values for σ and δ of –0.33 and 0.068, respectively, at a wavelength of 1550 nm in GaAs have been estimated at room temperature and shown to fit the experimental data very well.

Acknowledgment

The authors would like to thank Dan Kilper of Bell Laboratories, Crawford Hill, for helpful discussions. This work was supported by SFI under its CSET Centre for Telecommunication Value Driven Research (CTVR), Grant 03/CE3/I404 and by an SFI frontiers grant RFP/2006/ENE012.

#98727 - $15.00 USD Received 11 Jul 2008; revised 6 Oct 2008; accepted 6 Oct 2008; published 17 Oct 2008